Journal of Sound and Vibration (2001) **245**(4), 701–714
doi:10.1006/jsvi.2001.3561, available online at http://www.idealibrary.com on IDEAL®

PASSIVE VIBRATION SUPPRESSION OF BEAMS AND BLADES USING MAGNETOMECHANICAL COATING

H.-Y. YEN AND M.-H. HERMAN SHEN

Department of Aerospace Engineering, Applied Mechanics and Aviation, The Ohio State University, 328, *Bolz Hall*, 2036 *Neil Ave Columbus, OH* 43210-1276, *U.S.A. E-mail: shen.1@osu.edu*

(*Received* 13 *September* 1999, *and in final form* 2 *January* 2001)

The feasibility of using magnetomechanical coating for enhancing high damping capacity on turbine blades is investigated. An analytical procedure is developed for modelling the dynamic behavior of beams and blades coated with a plasma-sprayed iron–chromium-based coating. The stress- or strain-dependent damping capability of the coating material is evaluated experimentally and further quantified with a distribution function proposed by Smith and Birchak (1968 *Journal of Applied Physics* **39**, 2311–2316 [1], 1969 *Journal of Applied Physics* **40**, 5174–5178 [2]). The equation of motion and associated boundary conditions are derived for uniformly coated beams. The resulting equation of motion is solved for beams using a closed-form procedure. To validate the closed-form solutions and further investigate the effects of a thin coating on high-frequency chordwise bending modes or stripe modes (the terminology widely used by the turbine engine industry) of the vibrations of a curved blade, a three-dimensional finite element approach is used, which allows one to systematically determine the stress-dependent damping properties. The finite element results show that a thin magnetomechanical coating layer can make a significant contribution to the damping and reduction of vibratory or alternating stresses at various high-frequency vibration stripe modes.

1. INTRODUCTION

Many load-carrying structural systems, such as aircraft gas turbine engines, typically operate under severe conditions. This type of structure demands durability, high reliability, light weight, and high performance. Traditionally, lifetime failure-free design criteria based on the Goodman Diagram and Miner's rule have been adopted by the aircraft engine design community for ensuring the safety of critical structural components.

These design criteria, design guides, or design codes are often established using the results of a simple deterministic analysis procedure, without taking into account such information as degradation of material properties, scatter in test data, previous successful design experience, and uncertainties inherent in real-world operating conditions. In turn, as has been reported, a number of structural failures have occurred in aircraft engines during development testing and operational service. These incidents triggered an awareness of the fact that although current aircraft engine critical structural components satisfy the lifetime failure-free design criteria, they sometimes fail, blading systems in particular. Therefore, preventing turbomachinery blade failures is one of the major objectives of current aircraft engine design.

These failures generally result from high vibratory stresses in various stage turbomachinery blades during resonant response. Resonant response occurs in a non-uniform flow field operating environment when the excitation frequency from unsteady aerodynamic loading

0022-460X/01/340701 + 14 $35.00/0

is coincident with any blade's natural frequency. Hence, an adequate blade design would exist if all the resonant conditions could be avoided. Realistically, this is impossible due to the fact that insufficient real-world loading information is available at the time of the design.

To prevent blade failure, the excited resonant response needs to be attenuated to an acceptable level. Several investigators have presented approaches to suppress blade vibration by providing additional damping through blade dampers. For example, dry friction dampers [3] which include blade-to-ground, blade-to-blade, and shroud dampers are the most common vibration suppression devices employed by aircraft engine designers. However, it is well known that the structural damping from dry friction dampers and from aerodamping are negligible for high-frequency vibration; and the dominant damping of the blades results from the energy dissipation in the material. Consequently, low material damping results in high vibratory stress, increases failure risk, and significantly reduced reliability and safety [14]. This has motivated recent research studies of high-frequency dampers.

Recently, numerous investigations [5, 6] have been undertaken regarding the integration of viscoelastic damping materials into rotating blades for the purpose of reducing vibratory stresses in high-frequency stripe modes. The additional vibratory energy dissipation is accomplished through high internal friction in viscoelastic material patches inserted into milled cavities, which are sealed with a coversheet to maintain the structural integrity and the original airfoil contour. In addition to the temperature limitation of viscoelastic damping materials, such damping patches on blades lead to manufacturing and durability concerns. A surface high-damping coating layer is likely to be more practical.

Cross *et al.* [7] presented a method using several alternative candidate materials as graded plasma coatings on aluminum blades to obtain higher structural damping. Their test data demonstrated the use of three- to six-layered coatings of such materials as magnesium aluminate, molybdenum, and Hastelloy-X, to enhance the structural damping of the blades.

In this study, the objective is to explore the feasibility of using a magnetomechanical surface coating material [8] for increasing the high-frequency damping of turbine blades. The additional damping is achieved through internal friction via the magnetoelastic effects caused by stress or strain-induced irreversible movement of magnetic domain walls. According to the domain theory [9], the domain walls of the coating material rotate and generate a higher magnetic field strength under external loading. As the loading is removed, the domain walls rotate to a different pattern, which corresponds to a lower magnetic field strength. This process has been observed and shown to produce a significant amount of magnetomechanical hysteresis energy loss.

The strain or stress level dependence of the damping is discussed in section 2. In section 3, an analytical model for coating beams is presented. In section 4, a finite element approach on resonant response of coated beams and blades is presented. The finite element results are found to agree well with the closed-form solutions.

2. COATING MATERIAL

2.1. A BRIEF REVIEW OF ENERGY DISSIPATION MECHANISM [1, 2]

The energy dissipation mechanism due to the irreversible movement of magnetic domain boundaries has been studied by Smith and Birchak [1, 2]. They divided the energy dissipation density per cycle, ΔU_c, into two regions:

$$\Delta U_c = \frac{K\lambda}{\sigma_{loc}^2}\sigma^3 \quad \text{if } \sigma < \sigma_{cr}, \tag{1}$$

$$\Delta U_c = K\lambda\sigma_{loc} \quad \text{if } \sigma > \sigma_{cr}, \tag{2}$$

where K is a constant depending on the shape of the hysteresis loop, λ is the saturation magnetostriction, σ is the vibratory stress, σ_{loc} is the local internal stress, and σ_{cr} is the stress corresponding to the saturation point of the domain walls irreversible movement.

Later, using a probabilistic distribution, Smith and Birchok [1, 2] reformulated equations (1) and (2) to give

$$\Delta U_c = K\lambda\sigma_i\{1 - e^{-2s}(1 + 2s + 2s^2)\}, \tag{3}$$

where σ_i is the average internal stress, and s is defined by

$$s = \frac{\sigma}{\sigma_i} = \frac{\varepsilon}{\varepsilon_i}.$$

Therefore, the loss factor (η_c) of the coating material defined by

$$\eta_c = \frac{\Delta U_c}{2\pi U_c}, \tag{4}$$

can be represented as

$$\eta_c = \frac{K\lambda E}{\pi\sigma_i}[1 - e^{-2s}(1 + 2s + 2s^2)]/s^2, \tag{5}$$

where E is the Young's modulus and U_c is the vibratory energy density of the coating material.

2.2. DAMPING MEASUREMENT OF THE COATING MATERIAL

The above energy dissipation concept is applied to examine the effects of the coating damping on the forced response of beams and blades. Simply supported and cantilevered beams coated with a 10% beam thickness coating on the top surface are considered, as shown in Figure 1. The bending rigidity, $EI(1 + i\eta)$, of the coated beam is calculated from the RKU equation [10],

$$EI(1 + i\eta) = E_s I_s\left\{(1 + i\eta_s) + e_2 h_2^3(1 + i\eta_c) + 3(1 + h_2)^2\left[\frac{e_2 h_2(1 + i\eta_c)}{1 + e_2 h_2(1 + i\eta_c)}\right]\right\}, \tag{6}$$

where

$$e_2 = E_c/E_s, \qquad h_2 = h/d \tag{7}$$

and η_c is the loss factor of the coating material, h is the thickness of the coating layer, $2d$ is the thickness of the beam, and $E_s I_s(1 + i\eta_s)$ is the complex bending rigidity of the uncoated portion of the beam.

In accordance with ASTM standard E756-93 [11], a Ti-6Al-4V test beam and a steel test beam were machined, having dimensions 7·087 in × 0·3937 in × 0·079 in. A sinusoidal signal produced by a signal generator and amplified by a power amplifier was used to drive a dynamic shaker, exciting one end of the beam with the other end of the beam fixed. The

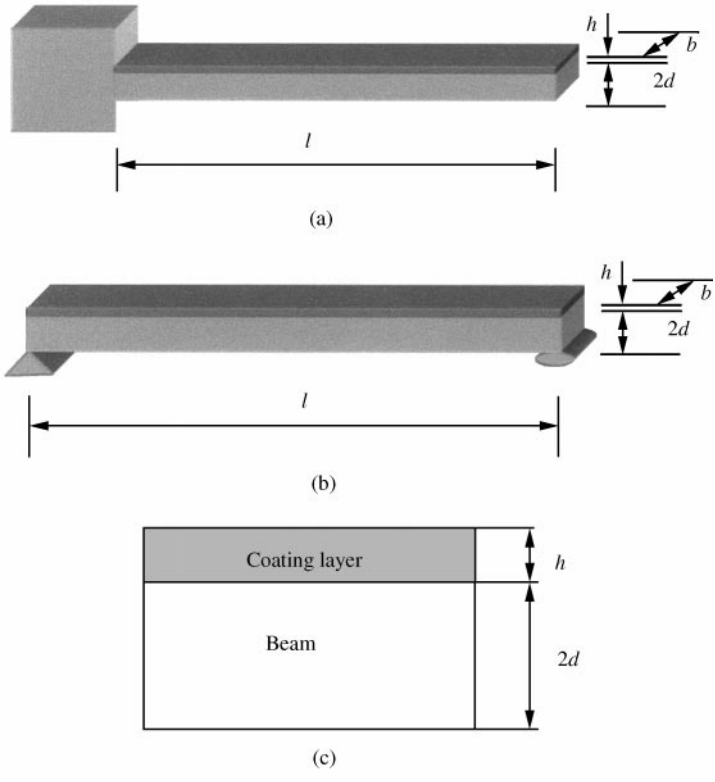

Figure 1. The geometry of the coated beams: (a) cantilevered beam, (b) simply supported beam, (c) beam cross section.

frequency was swept from 10 Hz to 10 kHz. The sinusoidal excitation input, acceleration, was measured by an accelerometer mounted just above the fixed end of the beam, and the output was determined via a laser vibrometer at the free end of the beam. The input and output signals were employed to produce the frequency-dependent transfer function. The damping loss factors of the first four vibration modes of the beams were calculated using the half power point method. Following this procedure, the loss factors of the steel and Ti-6Al-4V beams were found to be (approximately) 0·003 and 0·002 respectively.

A steel plate of dimensions 5·118 in × 3·937 in × 0·79 in coated with a 0·079 in thickness coating was cut into beams, and the resulting beams were tested similarly to the uncoated beams. The upper surface strain at the fixed end of the beam was calculated from simple beam theory, based on the deflection at the end of the beam as measured by the laser vibrometer. The damping loss factor was determined over a wide range of strain levels ($0–4 \times 10^{-4}$) from the frequency response function of the coated beam using the half power point method at the first vibration mode. Then the damping loss factor η_c, as shown in Figure 2, of the coating layer was calculated using the Ross–Kerwin–Ungar equation, equation (6).

Once the damping loss factor η_c of the coating layer is determined, damping properties ($K\lambda$), and the internal stress (σ_i) of the coating material can be obtained by fitting the loss factor function of equation (5) in a least-squares sense to the test data over the strain amplitude range that was investigated. Although any vibration mode response can be used to evaluate the damping properties, only the fundamental was considered here for simplicity.

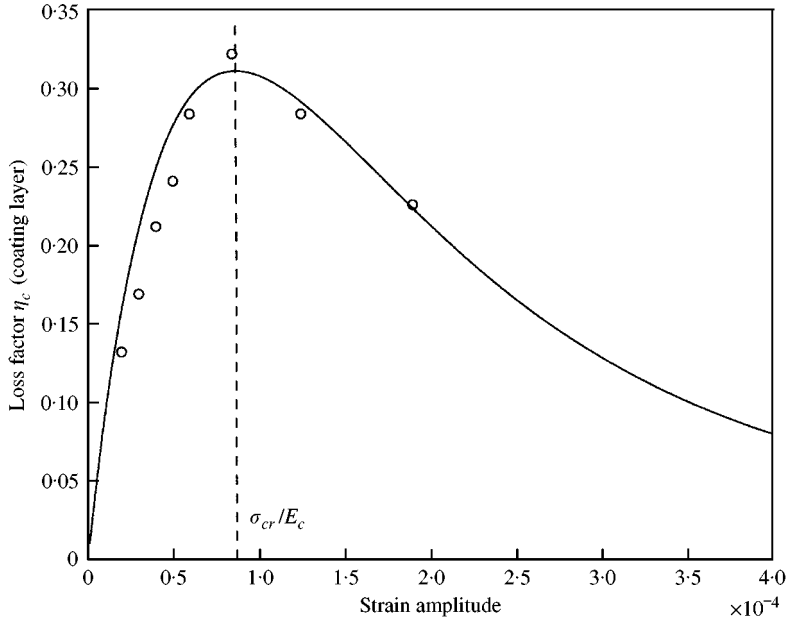

Figure 2. The comparison of curve fitting and test results: ○, test results; ——, curve fit.

The dependence of the damping loss factor on strain amplitude is shown in Figure 2. The least-squares fit between the testing data and loss factor determined the damping properties ($K\lambda$) and the internal stress (σ_i) to be 0·36, and $2{\cdot}5 \times 10^3$ psi respectively. Since the damping properties are observed to be stationary at high strain range, only a strain amplitude up to 4×10^{-4} was considered in the least-squares procedure. A least-squares procedure that leads to better agreement for high strains could have been performed, but then a discrepancy would occur for small strains. Thus, the least-squares fit chosen here is believed to be a good compromise because it leads to excellent results for strains up to 4×10^{-4}, while large strains are of no practical importance, since noticeable magnetomechanical damping would only occur at lower amplitudes.

Finally, it has been shown in equation (3) that the loss factor or the energy dissipation density per cycle of the coating material is independent of the vibratory frequency.

3. THEORETICAL DEVELOPMENT

3.1. KINEMATIC ASSUMPTIONS

We assume that the energy dissipation density of the coating per cycle can be characterized by the function of equation (3). Using this function, the energy dissipation through the coating layer can be expressed as

$$\Delta U_c = \int_0^l \int_{d/2}^{d/2+h} K\lambda\sigma_i[1 - e^{-2s}(1 + 2s + 2s^2)]\,dz\,dx. \tag{8}$$

If the thickness of the layer is small in comparison with the thickness of the blade, the lower surface strain of the coating layer is assumed to be the same as that of the upper beam

surface, which can be written as $\varepsilon = (d)w''$. It means that the overall thickness of the coated beam $2d + h$ can be replaced by the thickness of the uncoated one $2d$ during the computation. Hence,

$$e^{(d+h)w''/\varepsilon_i} \approx e^{(d)w''/\varepsilon_i}. \tag{9}$$

Then, replacing $(d + h)w''$ by $(d)w''$, equation (8) can be simplified to

$$\Delta U_c = \int_0^l \frac{K\lambda\varepsilon_i h E_c}{2\pi}\left[1 + \left(2 - \frac{(h+2d)w''}{\varepsilon_i}\right)e^{2dw''/\varepsilon_i}\right]dx. \tag{10}$$

3.2. VARIATIONAL THEOREM

Using classical variational principles such as the Hu-Washizu principle [12], the energy expression for the entire coated beam can be formulated by taking into account the energy dissipation in the coating layer. This yields the functional

$$\Pi = \int_{t_1}^{t_2}\left\{\int_0^l\left[\frac{1}{2}EI(1+i\eta_s)w''^2 + \frac{K\lambda\varepsilon_i hE_c}{2\pi}\left[1+\left(2\right.\right.\right.\right.$$

$$\left.\left.\left.\left. - \frac{(h+2d)w''}{\varepsilon_i}\right)e^{2dw''/\varepsilon_i}\right] - \frac{1}{2}\rho b(2d)\dot{w}^2 - \frac{1}{2}\rho bh\dot{w}^2\right]dx\right\}dt, \tag{11}$$

where ρ is the mass density, ε_i is the internal strain, l is the length of the beam, $2d$ is the thickness of the beam, and h is the thickness of the coating layer.

The functional Π in equation (11) is stationary for the solution w. Therefore, the first variation of Π must be equal to zero, yielding

$$\delta\Pi = \int_0^l\left\{EI(1+i\eta_s)w''\delta w'' + \frac{K\lambda\varepsilon_i hE_c}{2\pi}\left[(-h+2d)\right.\right.$$

$$\left.\left. - \frac{(2hd+4d^2)w''}{\varepsilon_i}\right]e^{2dw''/\varepsilon_i}\delta w'' + \rho b(2d+h)\dot{w}\delta\dot{w}\right\}dx = 0. \tag{12}$$

After integration by parts, equation (12) becomes

$$\delta\Pi = EI(1+i\eta_s)w''\delta w'|_0^l - EI(1+i\eta_s)w'''\delta w|_0^l$$

$$+ \frac{K\lambda hE_c}{2\pi}\left[(-h+2d) - \frac{(2hd+4d^2)w''}{\varepsilon_i}\right]e^{2dw'''/\varepsilon_i}\delta w'|_0^l$$

$$- \frac{K\lambda hE_c}{2\pi}\left[-\frac{4hdw''}{\varepsilon_i} - \frac{4(h+2d)d^2w''w'''}{\varepsilon_i^2}\right]$$

$$e^{2dw''/\varepsilon_i}\,\delta w'|_0^l + \rho d(d+h)\dot{w}\delta w|_0^l + \int_0^l \Big\{ EI(1+i\eta_s)w^{iv}$$

$$+ \frac{K\lambda h E_c}{2\pi}\left[\frac{4(h+2d)d^2}{\varepsilon_i^2}(w''w^{iv}+w'''^2) + \frac{8(h+2d)d^3}{\varepsilon_i^3}w''w'''^2\right.$$

$$\left.+\frac{8hd^2}{\varepsilon_i^2}w'''^2 + \frac{4hd}{\varepsilon_i}w^{iv}\right]e^{2dw''/\varepsilon_i} + \rho b(2d+h)\ddot{w}\Big\}\delta w\,dx = 0. \tag{13}$$

Therefore, for arbitrary independent variations, the equation of motion and the associated boundary conditions are obtained for the coated beams:

$$EI(1+i\eta_s)w^{iv} + \frac{K\lambda h E_c}{2\pi}\left[\frac{4(h+2d)d^2}{\varepsilon_i^2}w''w^{iv}\right.$$

$$\left.-\frac{8(h+2d)d^3}{\varepsilon_i^2}w''w'''^2 + \frac{4d^2(3h-2d)}{\varepsilon_i^2}w'''^2 + \frac{4d(2d-h)}{\varepsilon_i}w^{iv}\right]e^{2dw''/\varepsilon_i}$$

$$-\omega^2\rho b(2d+h)w = 0, \tag{14}$$

$$EI(1+i\eta_s)w''\delta w'|_0^l = 0, \qquad EI(1+i\eta_s)w'''\delta w|_0^l = 0, \tag{15, 16}$$

$$\frac{K\lambda h E_c}{2\pi}\left[(-h+2d) - \frac{(2hd+4d^2)w''}{\varepsilon_i}\right]e^{2dw''/\varepsilon_i}\,\delta w'|_0^l = 0, \tag{17}$$

$$\frac{K\lambda h E_c}{2\pi}\left[-\frac{4hdw'''}{\varepsilon_i} - \frac{4(h+2d)d^2w''w'''}{\varepsilon_i^2}\right]e^{2dw''/\varepsilon_i}\,\delta w'|_0^l = 0, \tag{18}$$

$$\rho b(2d+h)\dot{w}\delta w|_0^l = 0, \tag{19}$$

where ω is the natural frequency. Clearly, if there is no coating layer, the coating parameters $K\lambda$ are zero, and the equation of motion reduces to that of a uniform Bernoulli–Euler beam equation.

4. APPLICATION TO BEAMS AND BLADES

The effects of coating on the forced response of simply supported and cantilevered beams were studied. Results were obtained for the lowest three vibration modes by a closed-form procedure [13], using the collocation method [14], and by finite element computations.

The finite element approach also was applied to examine the forced response of coated blades at high-frequency third-stripe modes as shown in Figure 3. Approximately 10 000 four-node isoparametric and eight-node solid elements were used to model the coating layer and the blade. The number of elements was chosen to capture the effect of the coating on stripe modes at the frequency range of 3k–20kHz. To cover the fluctuating vibratory stress pattern, the coating is applied to the entire pressure side of the blade and modelled with two-dimensional isoparametric elements. It was demonstrated numerically that the finite element mesh shown in Figure 3 gives a convergent result for the present problem. Results for the high-frequency third-stripe mode have been obtained and evaluated.

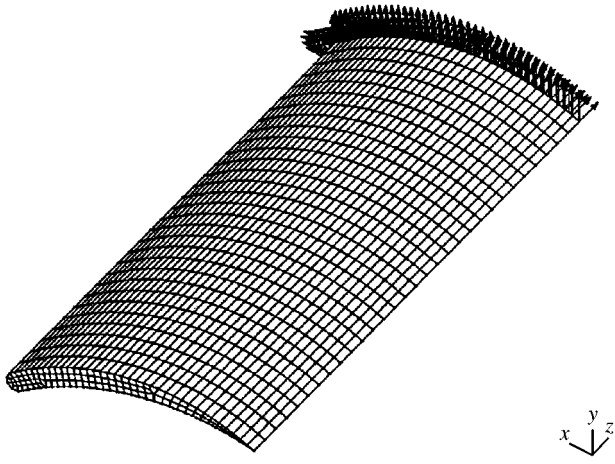

Figure 3. The finite element mesh of the turbine blade.

4.1. EFFECT OF COATING ON FORCED RESPONSE OF SIMPLY SUPPORTED BEAMS

A beam of rectangular cross-section of dimensions 3·937 in × 0·3937 in × 0·039 in with a 0·008 in thick plasma-sprayed iron–chromium-based coating layer has been considered in this investigation. Each beam was excited by a 0·5 lb harmonic load. Since the harmonic loading is applied at the mid-span of the beam, no even-numbered mode vibrations appeared in the results.

The first and the third forced vibration mode responses of a simply supported beam with a coating layer were computed and compared to the responses from the uncoated beam. As presented in Table 1, the maximum displacement reduction in the third mode is significant, as much as 63% by finite element approximation and 55% from the closed-form solution. However, the first mode shape reduction is relatively low (29·8% in closed-form solution and 22·8% by finite element approximation). This result can be explained by noting that a high strain level (as high as 0·0033) is produced in the majority portion of the beam during the first mode vibration. Consequently, lower damping (0·004–0·068 in loss factor) was produced from the coating layer in the first mode. In turn, as shown in Table 2, the coating layer can only reduce the maximum stress by 18% for the first mode vibration.

On the other hand, since the majority of the beam under the third mode vibration is contributing the strain in the range of $0–1{\cdot}3 \times 10^{-4}$, a high damping (as high as 0·2872 in loss factor) is therefore achieved in the third mode. Similar to displacement, as shown in Table 2, the coating layer is able to reduce the maximum stress by 63% in the third mode vibration.

4.2. EFFECT OF COATING ON FORCED RESPONSE OF CANTILEVERED BEAMS

Similar to the simply supported beam case, a relatively small effect of the coating layer on the first mode response is observed. As expected, a much larger effect is achieved on the second and third vibration modes, with 91 and 84% reduction in the maximum displacement by finite element approximation and 87 and 76% by closed-form solution.

The displacement of the coated beam is highly damped at the second mode vibration. Finally, as shown in Table 2, the vibratory stress of the cantilevered coated beams has been reduced by 18% in the first mode, and 77 and 58% in the second and third modes respectively.

TABLE 1

The maximum deformation (*inches*) *of simply supported* (*SS*) *and cantilevered* (*CL*) *beams.* (*FEM*: *finite element results*; *CLF*: *closed-form results*)

Vibration mode	First (SS)	Third (SS)	First (CL)	Second (CL)	Third (CL)
Uncoated	0·272	0·0029	1·07	0·062	0·0031
Coated (CLF)	0·191	0·0013	0·81	0·008	0·0007
Reduction in %	29·8%	55%	24·3%	87%	76%
Coated (FEM)	0·210	0·0011	0·69	0·006	0·005
Reduction in %	22·8%	63%	15%	91%	84%

TABLE 2

The maximum stress (*ksi*) *of simply supported* (*SL*) *and cantilevered* (*CL*) *beams.* (*FEM*: *finite element results*; *CLF*: *closed-form results*)

Vibration mode	First (SS)	Third (SS)	First (CL)	Second (CL)	Third (CL)
Uncoated	106	4·3	66	20·4	4·8
Coated (FEM)	72	1·6	54	4·7	2·0
Reduction in %	32%	63%	18%	77%	58%

4.3. EFFECT OF COATING ON FORCED RESPONSE OF CANTILEVERED BLADES

A case study was also conducted to illustrate a general procedure for enhancing damping capability of gas turbine blades using magnetomechanical coating. The goal in this case study is to investigate the feasibility of using the magnetomechanical coating for enhancing damping at the third-stripe mode, as shown in Figure 4, which is typical of actual hardware high cycle fatigue vibrations for which traditional dampers have difficulty achieving the desired stress reduction.

The gas turbine blade is made of Ti-6Al-4V, having the following dimensions: 3·0 in wide $\times$ 7·0 in long and 0·4 in average thickness, as shown in Figure 3. The aspect ratio of the blade (1·75) was higher than some modern blade designs, but resulted in frequencies and mode shapes similar to a real blade. The thickness of the coating was chosen to be 0·016 in, which is about 4% of the blade's average thickness.

Even though adding the coating layer on the pressure side of blade can reduce displacement significantly, eliminating the high stress for high cycle fatigue prevention is of primary interest. Therefore, only stress distributions of the second-, third- and forth-stripe modes of coated and uncoated beams are presented and examined.

The Goodman diagram of the Ti-6Al-4V material in Figure 5 was constructed by Maxwell and Nicholas [15]. The Goodman diagram is used to form the failure criteria or failure boundary in the traditional high cycle fatigue turbine blading system design procedure. This design process consists of a structural dynamics analysis to determine natural frequencies and mode shapes at certain operating speed ranges and a stress analysis to calculate the dynamic stress distribution for identifying the maximum vibratory stress location or region under a series of given excitations.

Once the maximum stress for each vibration mode has been determined, high cycle fatigue assessment can be achieved by measuring the margin between the maximum

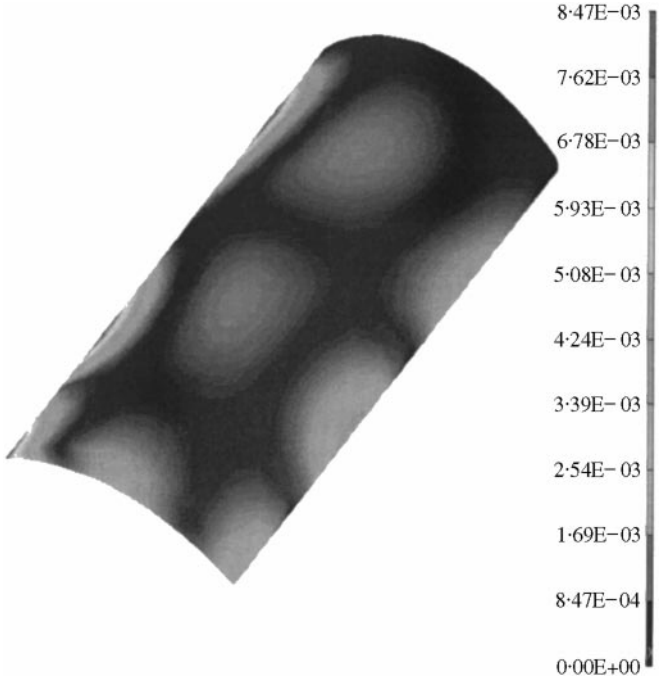

Figure 4. The third-stripe mode shape of the cantilevered blade at 10 676 Hz.

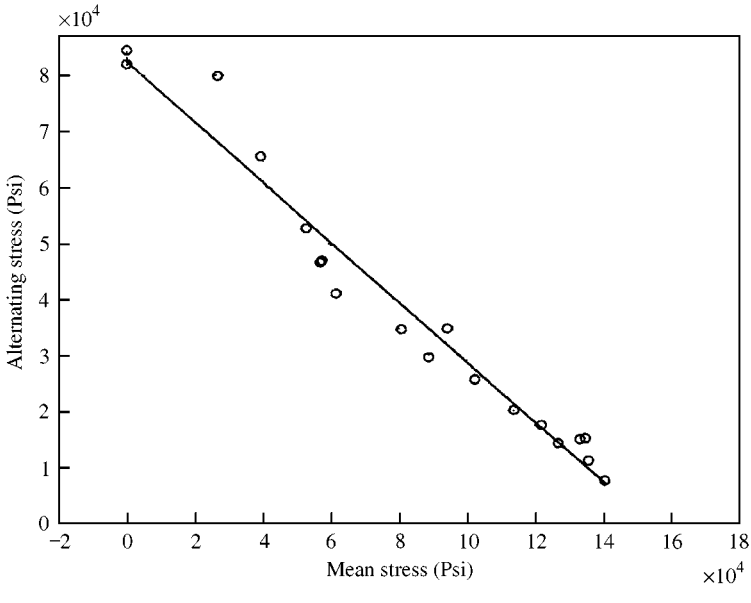

Figure 5. Haigh (or Goodman) diagram for Ti-6Al-4v.

vibratory stress and the material fatigue capability which is a typically straight line drawn between the mean ultimate strength at zero vibratory stress and the mean fatigue strength under fully reversed loading at 10^7 cycles (or infinite life) as shown in Figure 5. Therefore, in this study, a case study was conducted to illustrate how to attenuate the vibration stresses in

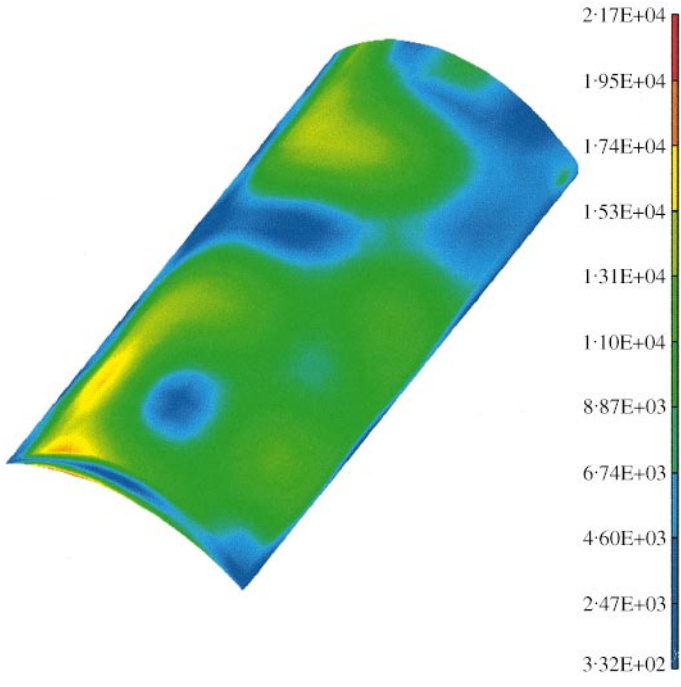

Figure 6. The von Mises stress in the third-stripe mode vibration of the cantilevered blade at 10 676 Hz (maximum von Mises stress 21·7 ksi; minimum von Mises stress 332 psi).

the three different stripe high-frequency vibration modes using the magnetomechanical coating damping.

Consider the case of the blade under a concentrated external harmonic excitation force applied at the tip portion of the blade. The magnitudes of the excitation force may be adjusted to achieve a maximum strain of 4×10^{-4}. Third-stripe mode von Mises stress distributions of coated blades excited by a 50 lb force on the central free end of the blades are computed and compared to those of an uncoated beam in Figures 6 and 7. Observe that the finite element results confirm the experimental predictions [7] that high vibratory stresses will be produced at high stripe modes.

One should note that the maximum vibratory stress, as expected, occurs near the trailing and clamped edges of the blade and shows significant reduction in comparison with uncoated blades. The drop in the von Mises stress is 17·6 and 9·4% at the second- and fourth-stripe modes, respectively, while a far greater drop to 42·9% occurs in the third-stripe mode. Similar to the beam case, the differences in stress reduction can be explained by noting that an adequate (in the sense of inducing coating damping) strain level or pattern is produced in the majority of the blade during the third-stripe mode vibration. Consequently, higher damping is therefore produced from the coating layer.

In accordance with the stress patterns presented in Figures 6 and 7, the maximum stress of the third-stripe vibration mode has been reduced to 42·9% by using only a 4% blade thickness magnetomechanical coating. This leads to the fact that even though the maximum stress of blade can be as high as 94 400 psi, the majority portion of the blade as shown in Figure 6 responds to a much lower vibratory stress level ranging from 400 to 6000 psi, which in fact is an ideal stress level for triggering the irreversible movement of magnetic domain boundaries of the coating material.

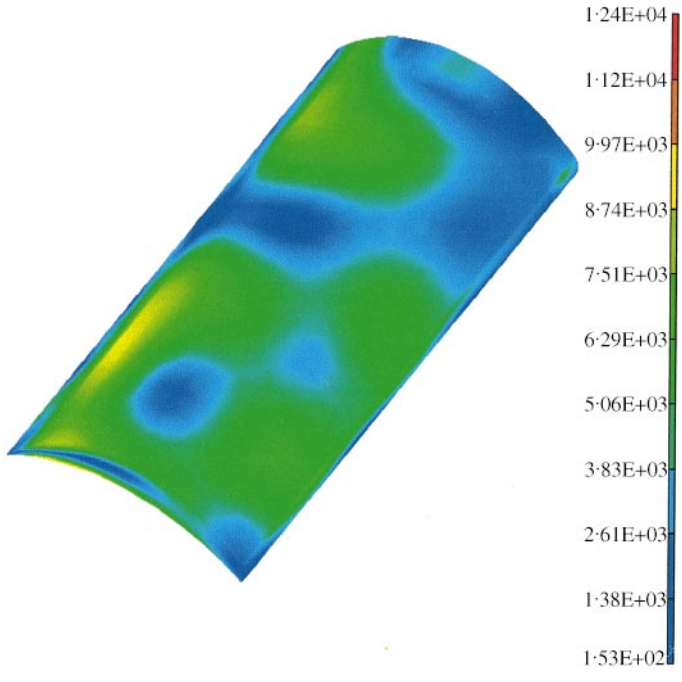

Figure 7. The von Mises stress in the third stripe mode vibration of the coated cantilevered blade at 9903 Hz (maximum von Mises stress 12·4 ksi; minimum von Mises stress 153 psi).

Several interesting observations can be made from the above discussions. First, for a certain loading condition, the maximum vibratory stress of the coated beam and blade can be significantly reduced at a specific mode and reasonably suppressed at other modes. Second, for a specific mode, the strain range or loading condition becomes a major factor for the coating damping capacity.

5. CONCLUSIONS

A new passive damping concept based on magnetoelastic effects from magneto-mechanical coating materials is proposed for vibratory stress and amplitude reduction on vibrating beams and blades. A model for the vibration of beams and blades containing a magnetic coating layer is presented. This is based on the magnetoelastic theory [1, 2], developed to formulate the mechanical energy dissipation from the irreversible movement of magnetic domain boundaries of the coating material.

The steady state response of the coated beams and blades is computed under a harmonic excitation force. The effect of the magnetic coating layer has been successfully examined and compared in the forced vibration analysis. The closed-form solutions and the finite element results show a significant vibratory stress and amplitude reduction of the vibrating beams and blades with a coating layer. The effects of the coating layer on the vibratory energy dissipation are found to be sensitive to the level of the strain or stress in the coating layer and independent of the vibration frequency. The present model could be easily extended to actual turbine blades with twisted non-uniform cross-section and can also account for the effects of centrifugal and thermo-loading.

ACKNOWLEDGMENTS

The authors wish to thank the reviewers for their valuable suggestions and comments.

REFERENCES

1. G. W. SMITH and J. R. BIRCHAK 1968 *Journal of Applied Physics* **39**, 2311–2316. Effect of internal stress distribution of magnetomechanical damping.
2. G. W. SMITH and J. R. BIRCHAK 1969 *Journal of Applied Physics* **40**, 5174–5178. Internal stress distribution theory of magnetomechanical hysteresis—an extension to include effects of magnetic field and applied stress.
3. J. H. GRIFFIN 1990 *International Journal of Turbo and Jet Engine* **7**, 297–307. Friction damping of resonant stresses in gas turbine engine airfoil.
4. M.-H. HERMAN SHEN 1999 *International Journal of Fatigue* **21**, 699–708. Reliability assessment of high cycle fatigue design of gas turbine blades using the probabilistic Goodman diagram.
5. R. W. GORDON and J. J. HOLLKAMP 1997 *AIAA/ASME/ASCE/AHS/ASC Structures, Structural Dynamics and Materials Conference*, Kissimmee, FL. Vol. VI, 442–451. Internal damping treatment for gas turbine blades.
6. R. KIELB, F. MACRI, D. OETH, P. MACIOCE, H. PANOSSIAN and F. LIEGHLEY 1999 *Proceedings (CD) of Fourth National Turbine Engine High Cycle Fatigue Conference, CA*. Advanced damping systems for fan and compressor blisks.
7. K. R. CROSS, W. R. LULL, R. L. NEWMAN and J. R. CAVANAGH 1973 *Journal of Aircraft* **10**, 685–687. Potential of graded coatings in vibration damping, an engineering note.
8. R. M. BOZORTH 1951 *Ferromagnetism*. Canada: D. Van Nostrand Co.
9. A. W. COCHARDT 1953 *Journal of Applied Mechanics* **20**, 196–200. The origin of damping in high-strength ferromagnetic alloys.
10. D. ROSS, E. E. UNGAR and E. M. KERWIN JR 1959 Damping Plate Flexural Vibrations by Means of Viscoelastic Laminate, Structural Damping, American Society of Mechanical Engineers, New York, pp. 49–88.
11. American Society for Testing and Materials (ASTM) 1993 *Standard test method for measuring vibration-damping properties of material*. ASTM E756-93. New York: American National Standards Institute.
12. K. WASHIZU 1982 *Variational Methods in Elasticity and Plasticity* Pergamon Press; Oxford: Third edition.
13. E. J. DOEDEL, A. R. CHAMPNEYS, T. F. FAIRGRIEVE, Y. A. KUZNETSOV, B. SANDSTEDE and X. WANG 1998 *AUTO 97, Canada*. Continuation and bifurcation software for ordinary differential equations.
14. U. M. ASCHER, R. M. M. MATTHEIJ and R. D. RUSSELL 1988 *Numerical Solution of Boundary Value Problems for Ordinary Differential Equations*. Englewood Cliffs, Prentice-Hall Inc.
15. D. C. MAXWELL and T. NICHOLAS 1998 *Fatigue and Fracture Mechanics*, Vol. 29, ASTM STP-1321. A rapid method for generation of a Haigh diagram for high cycle fatigue. American Society for Testing and Materials, West Conshohocken, PA.

APPENDIX A: NOMENCLATURE

E	Young's modulus of elasticity (coated beam)
E_c	Young's modulus of elasticity (coating material)
E_s	Young's modulus of elasticity (steel)
G	shear modulus of elasticity (coated beam)
I	moment of inertia (coated beam)
I_s	moment of inertia (uncoated beam)
$K\lambda$	magnetic parameters
U_c	strain energy density (coating material)
ω	free vibration natural frequency
c	width of the beam
$2d$	thickness of the uncoated beam
h	thickness of the coating layer

l	length of the beam
s	$\sigma_i/\sigma \equiv \varepsilon_i/\varepsilon$
ΔU_c	Energy dissipation density (coating material)
η	loss factor (coated beam)
η_c	loss factor (coating material)
η_s	loss factor (uncoated beam)
ρ	density (coated beam)
σ	vibratory stress
σ_i	average internal stress
σ_{loc}	local internal stress
σ_{cr}	critical stress on the saturation point
ε	vibratory strain
ε_i	average internal strain